



A short-TR single-echo spin-echo breath-hold method for assessing liver T2

Marshall S. Sussman¹ · Kartik S. Jhaveri¹

Received: 7 July 2023 / Revised: 27 October 2023 / Accepted: 28 October 2023 / Published online: 10 December 2023
© The Author(s), under exclusive licence to European Society for Magnetic Resonance in Medicine and Biology (ESMRMB) 2023

Abstract

Objective Conventional single-echo spin-echo T2 mapping used for liver iron quantification is too long for breath-holding. This study investigated a short TR (~100 ms) single-echo spin-echo T2 mapping technique wherein each image (corresponding to a single TE) could be acquired in ~17 s—short enough for a breath-hold. TE images were combined for T2 fitting. To avoid T1 bias, each TE acquisition incremented TR to maintain a constant TR-TE.

Materials and methods Experiments at 1.5T validated the technique's accuracy in phantoms, 9 healthy volunteers, and 5 iron overload patients. In phantoms and healthy volunteers, the technique was compared to the conventional approach of constant TR for all TEs. Iron overload results were compared to FerriScan.

Results In phantoms, the constant TR-TE technique provided unbiased estimates of T2, while the conventional constant TR approach underestimated it. In healthy volunteers, there was no significant discrepancy at the 95% confidence level between constant TR-TE and reference T2 values, whereas there was for constant TR scans. In iron overload patients, there was a high correlation between constant TR-TE and FerriScan T2 values ($r^2 = 0.95$), with a discrepancy of 0.6+/- 1.4 ms.

Discussion The short-TR single-echo breath-hold spin-echo technique provided unbiased estimates of T2 in phantoms and livers.

Keywords Iron Overload · Magnetic Resonance Imaging · Liver · Spin Echo Imaging

Introduction

Patients with hematological disorders such as thalassemia or myelodysplastic syndromes receive frequent blood transfusions for anemia correction [1]. Repetitive blood transfusions can cause systemic iron overload, with an excess deposition of iron in the liver, heart, pancreas, endocrine glands, and other tissues of the body. Liver iron concentration (LIC) is a good predictor of development of liver disease, and is used as a surrogate for total body iron [2]. Iron overload is mitigated with chelation therapy. However, the therapy itself can have toxic side effects. Thus, to monitor both the efficacy as well as possible toxicity of chelation therapy, it is essential to monitor liver iron concentration at regular intervals.

Chelation therapy may need to be modified with respect to dosage and/or chelating agent based on LIC trends [1].

MRI is currently the method-of-choice for monitoring LIC. It is non-invasive and can quantify the spatial distribution of iron throughout the liver. A variety of MRI methods are used to quantify LIC, including; signal intensity ratios [3], T2/T2* mapping [4–6] and QSM [7]. One of the most commonly used methods for LIC quantification is the T2-based FerriScan technique (Resonance Health Limited, Burswood, WA, Australia) [6]. It has been validated extensively, and has received regulatory approval. However, it does have some drawbacks: It does incur an added cost ~\$350 US per exam. Related to this, an additional administrative burden of a request for Government approval is required at some institutions (including our own). Cost considerations may also limit the frequency of testing. Additionally, there may be a delay in obtaining the LIC results since data must be sent offsite for post-processing and analysis. Institutional approval may also be required for external transfer of patient data. As a result, there is interest in developing alternative liver T2 quantification methods.

✉ Marshall S. Sussman
marshall.sussman@utoronto.ca

¹ Joint Department of Medical Imaging, University Health Network, Mount Sinai Hospital, and Women's College Hospital, University of Toronto, 585 University Avenue, Room NUW-1-141D, Toronto, ON M5G 2N2, Canada

The major challenge in performing T2 quantification in the liver is respiratory motion. Conventional spin-echo-based T2 mapping methods utilize TR times in the range of several seconds to permit near complete magnetization recovery. This results in a scan time of several minutes—far too long for a breath-hold. As an alternative, free-breathing scans with respiratory gating could be used. However, this generally results in excessively long scan times. FerriScan uses a free-breathing approach, but without gating. Instead, post-processing is used to remove respiratory-related artifacts [8]. In the early FerriScan protocol, even these non-gated free-breathing scans required about 20 min due to their long TR (= 2500 ms) [6]. FerriScan later introduced a short-TR (= 1000 ms) version of their protocol [9]. This reduced overall scan time significantly, though individual scans were still too long for breath holding (~2 min per TE). Respiratory artifacts were still removed through post-processing.

In the present study, we investigated a single-echo spin-echo technique with a TR that is short enough to be performed in a breath-hold. Similar to the FerriScan method, multiple single-echo spin-echo acquisitions were performed, each at a different TE. The data was combined to form a composite T2 decay signal. Unlike the FerriScan method, a short TR of ~100 ms was used so that the scan could be completed in a breath-hold. The challenge with using a short TR in a single-echo spin-echo pulse sequence is that magnetization recovery is incomplete during the TR. As a result, for each TE, there will be a variable amount of T1 recovery in the time between TE and TR. In turn, this biases the T2 fits [10]. In earlier work, we validated a technique that ensured a constant T1 recovery for all TEs [10]. The key to the technique was to use a TR that varied with the TE. In particular, the difference between TR and TE (i.e. the TR-TE value) was maintained constant. In the earlier study, in vivo experiments were performed in cartilage and brain using the constant TR-TE technique with a TR ~300 ms. In the present study, we assessed the constant TR-TE technique with a TR~100 ms. The motivation for going to this shorter TR was so that scans were short enough (~17 s) to be performed in a breath hold. The short TR single-echo spin-echo constant TR-TE technique was validated in phantoms, healthy volunteers, and iron overload patients.

Materials and methods

This prospective study was performed under Research Ethics Board approval at our institution. Written informed consent was obtained from all participants. Funding for this study was generously provided by GE Healthcare. Due to privacy concerns, data is not publicly available. All analysis was performed in Matlab.

Phantom experiments

Phantoms were constructed to provide T1 and T2 values similar to those found in the range of mild liver iron overload to healthy liver (T2~18–40 ms and T1~600–1000 ms) [6, 11, 12]. The challenge with constructing such phantoms is being able to independently control the T1 and T2 values. To accomplish this task, phantoms were constructed using the technique described by Tofts et al. [13, 14]. The phantoms consisted of agar (Sigma-Aldrich Canada) doped with MnCl₂. For a specific desired T1 and T2 value, Tofts et al. show that the required concentrations of Agar and MnCl₂ are given by:

$$C_{Agar} = \frac{1/T_2 - 1/T_{2_w} - (r_{2_p}/r_{1_p})(1/T_1 - 1/T_{1_w})}{r_{2_a} - (r_{2_p}/r_{1_p})r_{1_a}} \quad [\text{in}\%] \quad (1)$$

$$C_{MnCl_2} = \frac{1/T_1 - 1/T_{1_w} - (r_{1_a}/r_{2_a})(1/T_2 - 1/T_{2_w})}{r_{1_p} - (r_{1_a}/r_{2_a})r_{2_p}} \quad [\text{in mM}] \quad (2)$$

where T1_w, T2_w are the T1 and T2 values of water (in seconds); r1_a, r2_a are the longitudinal and transverse relaxivities of agar; and r1_p, r2_p are the longitudinal and transverse relaxivities of MnCl₂ (both in seconds⁻¹·mM⁻¹). Initial experiments using published values [13] of the above parameters were found to provide T1 and T2 close to, but not exactly equal to the desired values. Therefore, using these initial concentrations as a starting point, further trial and error was performed to achieve phantoms with the desired T1 and T2 values. Table 1 lists the final concentrations used for the phantoms. Ideally, it would be desirable to generate phantoms with even shorter T2 values corresponding to the range expected in moderate to high iron overload. However, according to Eq 1, this would have required even higher agar

Table 1 Agar and MnCl₂ concentrations used for the phantom construction, together with corresponding T2 (derived from the TR = 2500 ms reference scan) and T1 (derived from an inversion recovery sequence) values

Agar Concentration (%)	MnCl ₂ Concentration (mM)	T ₂ (ms)	T ₁ (ms)
10	0.127	17.3	503
9.1	0.100	17.7	768
10.2	0.019	18.8	1326
5.9	0.042	21.8	1157
5.0	0.122	23.3	702
5.0	0.127	24.3	589
3.9	0.067	32.1	1030
2.8	0.135	38.9	632

concentrations than those listed in Table 1. Unfortunately, it was not possible to achieve agar concentrations greater than ~10%. In fact, even the 10% concentration required heating on a hot plate to increase solubility.

The phantoms were imaged on a 1.5T GE Signa HDxt Scanner (GE Healthcare) using the transmit/receive quadrature head coil. Individual acquisitions at TEs of 6, 9, 12, 15, and 18 ms were performed (see Table 2). These TEs were selected to match those employed by FerriScan. For each separate TE scan, the TR was set appropriately to maintain a constant TR-TE value (i.e. TR = 106 ms for TE = 6 ms, TR = 109 ms for TE = 9 ms, etc.) [10]. T2 fitting was then applied to this complete TE data set. To test the performance of this technique in different TR ranges, these T2 acquisitions were repeated with four different TR-TE values (= 100, 200, 400, and 1000 ms). For comparison, scans using the same TEs, but with the conventional approach of maintaining a constant TR (= 100, 200, 400, and 1000 ms) were also acquired (i.e. TR = 100 ms for TE = 6 ms, TR = 100 ms for TE = 9 ms, etc.). Each individual acquisition with TR≈100, 200, 400, 1000, and 2500 ms took approximately 19, 33, 60, and 140 s respectively (see Table 2 for exact values). To provide a reference standard for the phantom experiments, an additional set of constant TR scans was performed using the same TE data set with a long TR of 2500 ms to allow for near full magnetization recovery. This scan took 350s. Other parameters included a matrix size of 128 × 128, slice thickness of 5 mm, BW = 62.5 KHz, and FOV = 30 cm.

For the healthy volunteer experiments (described later), it was not possible to use a long TR scan as a reference standard (due to respiratory motion). Therefore, a short-TR multi-echo spin-echo protocol was also validated on the phantoms for use as a reference on the healthy volunteers. Since all TEs were acquired during a single TR period, there were no T1 biasing effects like in the single-echo spin-echo case [10]. To maintain a similar TE range as the single-echo protocol, five echoes with an inter-echo spacing of 5.5 ms (the minimum possible) were used (see Table 2). As with the single-echo protocols, TRs of 100, 200, 400 and 1000 ms were used. Other parameters were similar to the single-echo spin-echo protocol, with the exception of a 31.25 KHz BW. Exact scan times are listed in Table 2.

For all scans used in this study, 90° excitation and 180° refocussing pulses were used.

To estimate noise, three acquisitions at the longest TE were performed for the single-echo scans, and all multi-echo scans were performed 3 times. For the latter, only the longest TE images were used for noise calculations. Noise was calculated as the standard deviation across the repeated longest TE images at a location in the background. Note that the noise calculations indicated that SNR>5 in all cases. Therefore, non-Gaussian noise statistics on the magnitude images did not have to be taken into account [15]. To calculate T2, a linear fit (using the “fit” command in Matlab) to the logarithmically-transformed decay data was performed by minimizing the reduced χ^2 value:

$$\chi_{reduced}^2 = \sum_{i=1}^n \left(\frac{y_i^{fit} - y_i^{measured}}{\sigma / y_i^{measured}} \right)^2 / DOF \quad (3)$$

where y_i^{fit} , $y_i^{measured}$ are the fitted and measured logarithmically transformed T2 decay signals, σ is the noise, and DOF is the number of degrees-of-freedom in the fit. Note that a weighted χ^2 value is used to account for the logarithmic transformation [16].

Linear regression was performed between the T2 values of all techniques and the TR = 2500 ms reference. Intercepts and slopes were compared to zero and unity respectively with a *t*-test. Significance was set at the 95% confidence level.

Healthy volunteer experiment

Nine healthy volunteers with no suspected iron overload (4 male, 5 female, mean age = 31, age range = 21–56) were scanned on a 1.5T GE Signa HDxt Scanner (GE Medical Systems) using the 8-channel body coil. Single-echo spin-echo acquisitions were performed with TEs the same as the phantom experiments. A single axial slice at the level of the porta hepatis was acquired. Relevant pulse sequence parameters included a matrix size of 128 × 128, FOV of 35 cm, and slice thickness of 5 mm. TR was either fixed at 100 ms (constant TR case) or varied to maintain TR-TE = 100 ms (constant TR-TE

Table 2 Relevant pulse sequence parameter used for the phantom experiments

PULSE SEQUENCE TYPE	TE (ms)	TR (ms)
Single-Echo Spin-Echo	6, 9, 12, 15, 18	TR-TE = 100, 200, 400, 1000 (19, 33, 60, 140 s)
		TR = 100, 200, 400, 1000, 2500 (17, 30, 58, 140 s)
Multi-Echo Spin-Echo	5.5, 11, 16.5, 22, 27.4	TR = 100, 200, 400, 1000 (15, 28, 54, 130 s)

The bracketed values correspond to the scan times for each TR. In the case of the constant TR-TE data, scan times correspond to the longest TE acquisition (the other TEs are slightly lower)

case). Breath-hold duration was between 17 and 19 s. As discussed earlier, a multi-echo spin-echo acquisition was also acquired for use as a reference in the healthy volunteers. For the multi-echo protocol, five echoes with an inter-echo spacing of 6.3 ms (the minimum achievable) was used to maintain a similar TE range as the single-echo protocol. A TR of 133 ms was used, resulting in a breath-hold duration of 17s. Superior and inferior saturation bands were used in all acquisitions to minimize the blood signal.

An ROI encompassing the entire liver was selected manually using Matlab. The ROI was chosen conservatively to avoid tissue borders, and exclude larger (~7 mm or greater) blood vessels. Pixelwise T2 fitting was performed in a similar manner to the phantom scans, and the median T2 value calculated over all pixels in the ROI. The median was used because it is less sensitive to outlier caused by potential fit failures (due to artifacts, motion, etc.). Normality of the median liver T2 values across volunteers was assessed with an Anderson-Darling test. The median liver T2 values between multi-echo, constant TR-TE, and constant TR scans across volunteers were compared with a Tukey-Kramer multiple comparison test. The median discrepancy between individual pixel T2 values of each of the single-echo techniques, and the multi-echo reference scan was also calculated. The χ^2 fit values were compared with a paired Student-t test. Significance was set at the 95% confidence level.

Iron overload patients

Five patients (3 male, 2 female, mean age = 45, age range = 35–56) with confirmed iron overload were scanned on a 1.5T Avanto Fit scanner (Siemens). Standard FerriScan and constant TR-TE acquisitions were performed. The constant TR-TE scans used similar parameters as in the healthy volunteers, with the exception that four 5 mm slices were acquired with a gap of 5 mm. Four slices were used, as this was the maximum allowable within the TR period. These were prescribed from the central slices of the FerriScan acquisition (which itself consisted of 11 slices).

The T2 values derived from the FerriScan reports were used as the reference standard. To provide as fair a comparison as possible to this reference, the post-processing performed on the constant TR-TE data was similar to the FerriScan protocol as described in Refs. [6, 9, 17, 18]. In particular, images were post-processed to correct for signal drift, noise bias, and low-pass filtered to improve SNR. Since our images were acquired in a breath hold, unlike FerriScan, post-processing correction for ghosting artifacts was *not* performed. Pixelwise fitting was performed using a Levenberg-Marquardt algorithm to the following bi-exponential model:

$$S(TE) = S_f(TE = 0)e^{-r_{2f} \cdot TE} + S_s(TE = 0)e^{-r_{2s} \cdot TE} \quad (4)$$

where “S” indicates the signal, and the “f” and “s” subscripts indicate the fast and slow compartments respectively. As per the FerriScan protocol [6, 9, 17, 18], an average relaxation rate for the system was calculated as:

$$R_{2_{av}} = \rho_f \cdot r_{2f} + \rho_s \cdot R_{2s} \quad (5)$$

where:

$$\rho_f = \frac{S_f(0)}{S_f(0) + S_s(0)}, \rho_s = \frac{S_s(0)}{S_f(0) + S_s(0)} \quad (6)$$

Finally, the average T2 value was calculated for each pixel as:

$$T_{2_{av}} = 1/R_{2_{av}} \quad (7)$$

Mean $T_{2_{av}}$ values were calculated over whole liver ROIs from all four slices (again using Matlab to manually draw the ROIs), excluding larger blood vessels. These were compared to $T_{2_{av}}$ values calculated from the FerriScan reports. A linear fit was performed between the constant TR-TE and FerriScan values. Slope and intercepts were compared to unity and zero respectively with a *t-test*. Significance was set at the 95% confidence level. A Wilcoxon Rank-Sum test was used to compare the coefficient-of-variation between constant TR-TE and FerriScan techniques.

Results

Phantom experiments

Figure 1 consists of T2 maps of the phantom from the shortest TR acquisitions (~100 ms) as well as the long TR reference standard. The multi-echo and constant TR-TE T2 values are consistent with the reference. However, the constant TR T2 maps underestimate the T2 values; especially for the longer T2 vials. Note that in all cases, the SNR of the 100 ms acquisitions is clearly lower than the long TR reference (as expected).

Figure 2a plots example T2 decay curves, together with monoexponential fits for one of the phantoms. Qualitatively, the similarity between the constant TR-TE = 100 m and long TR = 2500 ms reference fits can be observed, while the TR = 100 ms appears to decay away more quickly. Quantitatively, Fig. 3 compares the T2 values of the short TR sequences to the long TR reference standard. Both the constant TR-TE and constant TR pulse sequences exhibit a linear relationship that is highly correlated (i.e. high r^2 values) with the reference TR = 2500 ms values. The results of linear fitting (Table 3) indicate a slope of unity and an intercept of zero for the constant TR-TE data at all TR values. The constant TR data, on the other hand, has a non-unity slope and/or

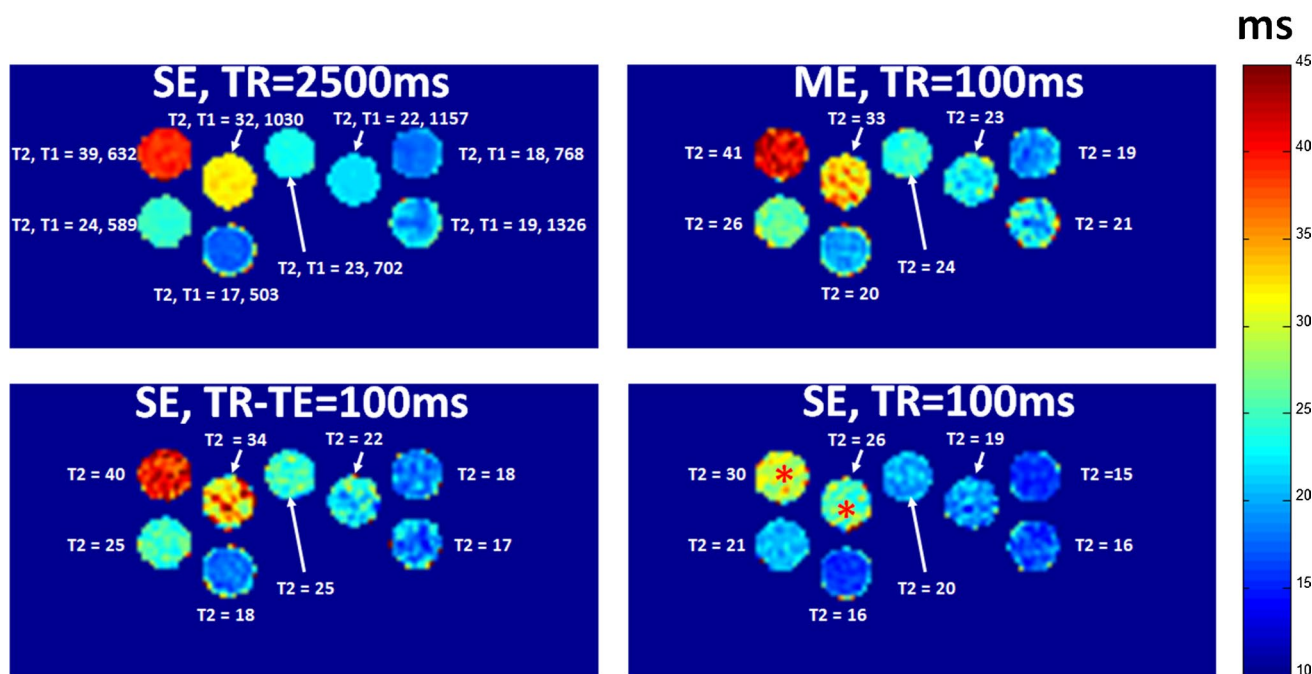


Fig. 1 Phantom T2 maps acquired with single-echo (SE) and multi-echo (ME) scans. The T2 and T1 values associated with the scans are indicated in the figure (in ms). Note that the vials with the longest T2 values in the constant TR=100ms case (red “*’s”) exhibit the large-

est discrepancy with the TR=2500ms reference T2 map. The discrepancy is lower for the other two T2 maps (ME, and constant TR-TE = 100 ms)

a non-zero intercept for TR values ≤ 400 ms. It tends to underestimate the reference T2 value. These observations can also be inferred from the Bland-Altman plots in Fig. 4.

Figure 3 also plots the results from the multi-echo scans that will be used as a reference on the healthy volunteers. The multi-echo data is highly correlated with the reference TR = 2500 ms values. However, while the slope is unity, the intercept is non-zero (Table 3 and Fig. 4).

Healthy volunteer experiments

Figure 2b plots example T2 decay curves, together with monoexponential fits for one of the healthy volunteers. The similarity between the constant TR-TE = 100 ms and multi-echo reference fits can be observed. The constant TR=100ms signal, however, clearly different. Similar to the phantom data, it underestimates the T2 value relative to the reference (i.e. more rapid decay).

Figure 5 illustrates T2 maps from two volunteers. The consistency between the multi-echo and constant TR-TE techniques can be observed. On the other hand, the constant TR technique T2 values are lower. Also note that relatively large overall heterogeneity in the T2 maps. This is due to the relatively low SNR when using short TRs.

Figure 6 plots the median liver T2 values of the constant TR-TE and constant TR acquisitions versus the

multi-echo reference. Qualitatively, the similarity between the multi-echo and constant TR-TE data can be observed. The constant TR data, on the other hand, exhibits both a larger discrepancy with the other two acquisitions, as well as a larger scatter. Quantitatively, the mean T2 values over all volunteers was: 41 ± 3 , 33 ± 9 , and 41 ± 3 ms for constant TR-TE, constant TR, and multi-echo scans respectively. The Andersen-Darling test indicated that the median T2 values were normally distributed for multi-echo, constant TR-TE, and constant TR data ($p = 0.92$, 0.44 , and 0.80 respectively). The results of the Tukey-Kramer multi-comparison analysis found no significant discrepancy between the median liver ROI T2 values of multi-echo and constant TR-TE scans at the 95% confidence level. Conversely, significant discrepancy was found with both multi-echo and constant TR-TE techniques relative to the constant TR liver ROI T2 values.

The discrepancy between individual pixels of multi-echo and constant TR-TE images was -0.20 ± 2.10 ms (median \pm standard deviation). The discrepancy between multi-echo and constant TR images was -7.07 ± 7.48 ms.

There was no significant difference in the χ^2 values of the constant TR-TE ($= 3.8 \pm 2.7$) and constant TR ($= 3.8 \pm 2.7$) at the 95% confidence level ($p = 0.90$).

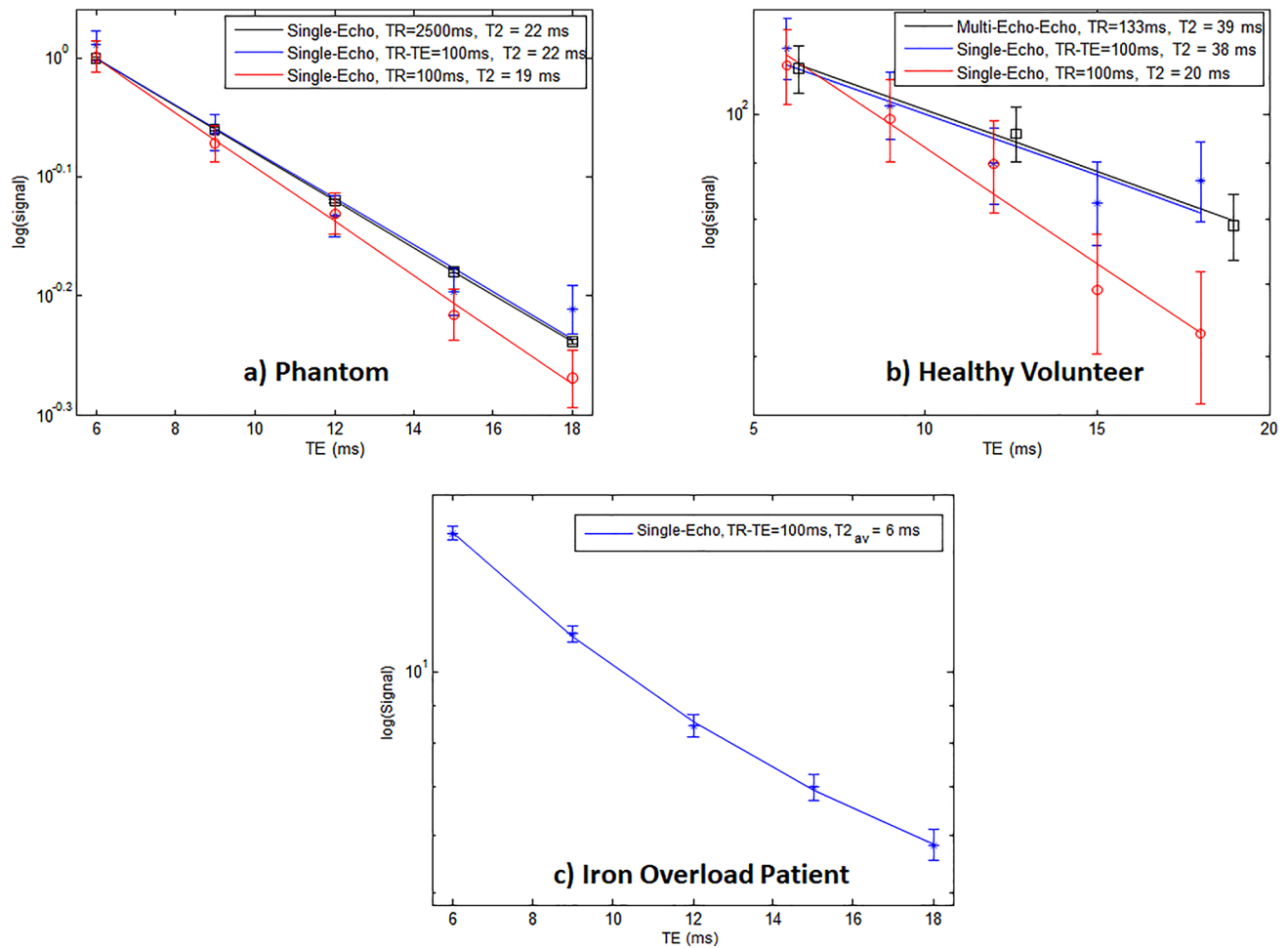


Fig. 2 Example T2 decay curves (log signal versus time) together with corresponding fits for a) phantom, b) healthy volunteer, and c) iron overload patient experiments. Phantom and volunteer fits are monoexponential, whereas the iron overload patient fit is bi-exponential. The FerriScan report indicated an iron load of 14 mg Fe/g dry

Iron overload patients

Figure 2c plots example T2 decay curves, together with the biexponential fit for one of the iron overload patients. Figure 7 illustrates T2 maps from two iron overload patients. Note that these maps appear to have a higher SNR than the healthy volunteer T2 maps (Fig. 5). This is because, unlike the healthy volunteer data, the iron overload patient data employed low-pass filtering (done to maintain consistency with FerriScan). Figure 8 plots the mean liver T2_{av} values of the constant TR-TE technique against the T2_{av} values derived from the FerriScan reports. The fitted T2_{av} values range from 6.0 to 20.3 ms. There is a high correlation between the two ($r^2 = 0.95$), with a discrepancy of 0.6 ± 1.4 ms. Regression fits indicate a slope not significantly different from unity ($p = 0.36$) and an intercept not significantly different from zero ($p = 0.52$) at the 95% confidence level. The coefficient of

weight liver for this patient. Note that the phantom decay curves have been normalized to the signal at the first TE due to the large difference in signal intensity between the long TR reference and short TR scans. Error bars represent the noise estimates

variation was 0.25 ± 0.05 and 0.19 ± 0.07 for constant TR-TE and FerriScan T2_{av} values. The Wilcoxon Rank-Sum test indicated no significant difference between these values ($p = 0.1$).

Discussion

This study investigated a short-TR single-echo spin-echo technique for breath-hold T2 mapping. The key to this technique was maintaining a constant TR-TE value. Phantom experiments demonstrated that this technique was well-correlated with the reference data, and provided an unbiased estimate of T2 using TRs down to 100ms. In comparison, the conventional approach of using a constant TR exhibited biases at shorter TR values. In particular, it tended to underestimate the true T2 value at shorter TRs. In healthy

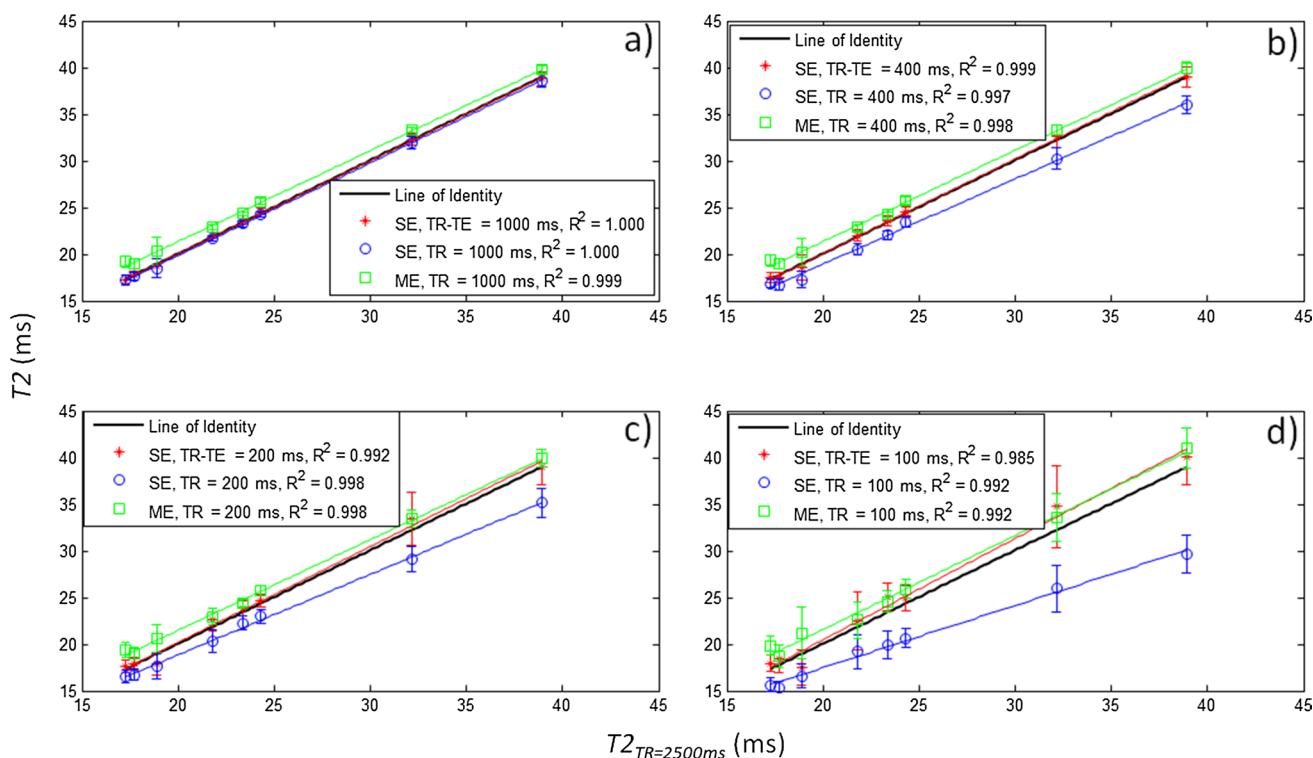


Fig. 3 Phantom results for single-echo (SE) constant TR-TE and constant TR, and multi-echo (ME) pulse sequences. Short TR T2 values are plotted against the single-echo spin echo long TR reference T2 values. Each subfigure represents the results from a different short TR

and TR-TE value: **a** TR and TR-TE = 1000 ms, **b** TR and TR-TE = 400 ms, **c** TR and TR-TE = 200 ms, and **d** TR and TR-TE = 100 ms. Error bars represent the standard deviation over the vial ROI

Table 3 Intercept and slope of the short TR scans relative to the long-TR reference for the phantom experiment. The square bracketed data represents the 95% confidence intervals, and the round bracketed data represents the p-value in the test for non-unity slope and non-zero intercept. “*” indicates statistical significance at the 95% confidence level

SEQUENCE TYPE	TECHNIQUE	INTERCEPT (ms)	SLOPE
Single-Echo Spin-Echo	TR-TE = 1000	0.10 [− 0.24, 0.43] (0.648)	1.00 [0.99, 1.01] (0.843)
	TR-TE = 400	− 0.18 [− 0.72, 0.35] (0.595)	1.01 [0.99, 1.03] (0.334)
	TR-TE = 200	− 0.31 [− 1.73, 1.11] (0.729)	1.03 [0.97, 1.08] (0.460)
	TR-TE = 100	− 1.10 [− 3.21, 1.01] (0.425)	1.08 [1.00, 1.16] (0.163)
	TR = 1000	0.03 [− 0.25, 0.31] (0.875)	0.98 [0.98, 1.00] (0.323)
	TR = 400	0.72 [− 0.12, 1.55] (0.206)	0.91 [0.88, 0.95] (0.005)*
	TR = 200	1.67 [1.02, 2.31] (0.005)*	0.86 [0.84, 0.89] (<10 ^{−3})*
	TR = 100	4.18 [3.23, 5.12] (<10 ^{−3})*	0.67 [0.63, 0.7] (<10 ^{−3})*
Multi-Echo Spin-Echo	1000	1.96 [1.41, 2.51] (0.001)*	0.97 [0.95, 0.99] (0.078)
	400	1.88 [1.22, 2.55] (0.003)*	0.98 [0.95, 1.00] (0.176)
	200	2.15 [1.47, 2.85] (0.002)*	0.97 [0.94, 1.00] (0.115)
	100	1.53 [0.09, 2.97] (0.131)	1.00 [0.95, 1.06] (0.903)

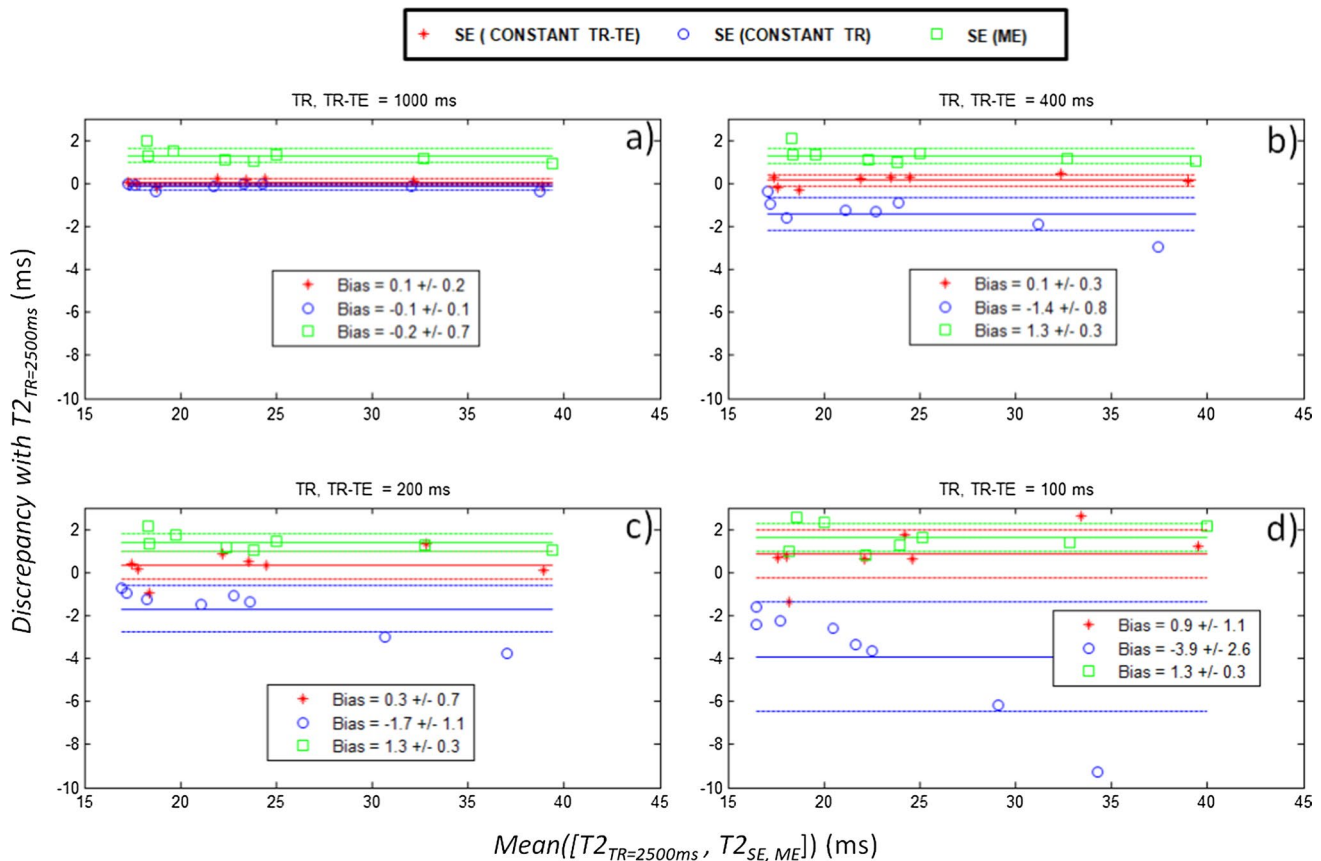


Fig. 4 Bland-Altman plots for phantom data for single-echo (SE) and multi-echo (ME) protocols. The vertical axis is the discrepancy between the short TR and long TR T2 values. The horizontal axis is the mean of the short and long TR T2 values. The solid lines represent the mean discrepancy, while the dashed lines represent the 95%

confidence intervals. Each subfigure represents the results from a different short TR and TR-TE value: **a** TR and TR-TE = 1000 ms, **b** TR and TR-TE = 400 ms, **c** TR and TR-TE = 200 ms, and **d** TR and TR-TE = 100 ms. The listed bias is the mean \pm standard deviation of the discrepancy

volunteers, the constant TR-TE technique provided equivalent liver T2 values to the reference, while the constant TR method generally underestimated it. There were no differences in the goodness-of-fit (i.e. χ^2 values) between the two techniques. In iron overload patients, there was a high correlation between the T2_{av} values calculated from the constant TR-TE technique and those derived by FerriScan. This high correlation was achieved despite the fact that iron distribution within the liver can be heterogeneous [6], and different liver ROIs were analyzed by our group and FerriScan.

As discussed in Ref. [10], the conventional constant TR approach requires that $TR \gg T1$ (i.e. full magnetization recovery). At short TRs, this condition is not satisfied, leading to the biases observed in this study for the constant TR technique. The constant TR-TE technique eliminates this requirement. However, this latter technique does have two additional requirements [10]: First, it requires that $TE/T1 \ll 1$. This condition will be easily satisfied for any realistic TE and T1 encountered in liver iron imaging. The second requirement is that $TR/T2 \geq 3$. This will certainly be

achieved at high iron loads, where T2 values will be less than 10ms and TRs are in the 100ms range. On the other hand, this requirement may not be fully met in the case of normal liver; where T2's are in the range of 35–45 ms. However, the results of this study indicate that accurate T2 mapping was achieved even in healthy volunteers using a TR in the 100 ms range (as well as in phantoms with T2's in this range). In fact, the constant TR-TE T2 values for healthy volunteers found in this study using the constant TR-TE technique ($= 41 \pm 3$ ms) were nearly identical to those found in a recent study ($= 41 \pm 5$ ms) using a radial TSE pulse sequence [19]. For comparison, the constant TR technique in this study provided liver T2 values of 33 ± 9 ms.

It should be mentioned that the TR value of ~ 100 ms used in this study was chosen somewhat arbitrarily simply to demonstrate the feasibility of performing breath-hold T2 mapping using TRs in that short range. Further optimization may be possible. For example, it may be possible to use even shorter TRs to achieve further reductions in scan time. However, this would have to be validated in light of

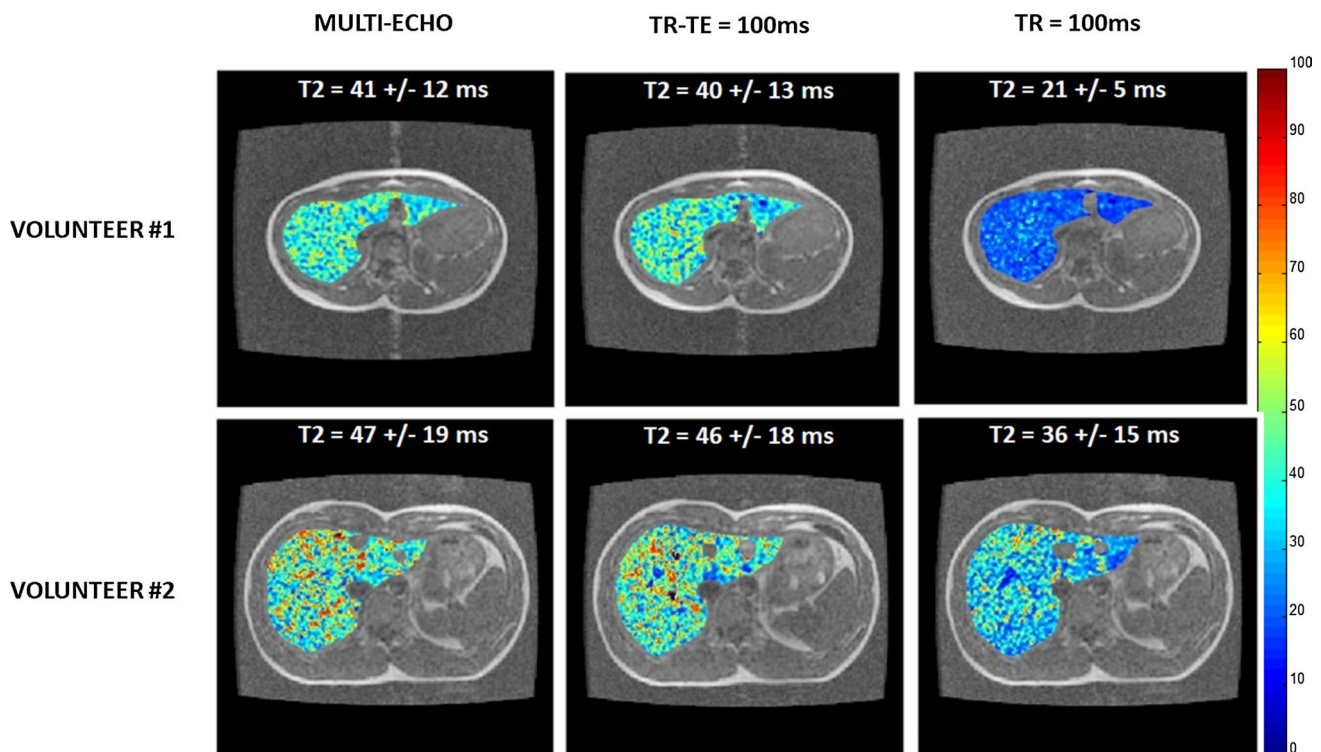


Fig. 5 T2 maps for multi-echo, constant TR-TE = 100 ms, and constant TR = 100 ms techniques for two volunteers. Listed T2 values represent the mean and standard deviation over the liver

the technique's constraints discussed in the previous paragraph, as well as SNR limitations. Another possibility is that acceleration or partial Fourier techniques could be employed (they were not in the present study) to permit a longer TR, whilst maintaining a similar scan time. Alternatively, accelerated imaging could also be utilized to improve resolution and/or reduce scan time relative to the current protocol [20]. Longer TRs and parallel imaging could also be varied to optimize SNR. In the present study, SNR was relatively low with the use of the short 100 ms TR. This can be seen in the healthy volunteer T2 maps. Low SNR was not as apparent in the iron overload T2 maps due to the use of low-pass filtering (done to maintain consistency with the FerriScan protocol). Despite the fact that FerriScan acquisitions used a much longer TR (= 1000 ms), there was no significant difference in the T2av coefficient-of-variation with the constant TR-TE scans. This suggests that variation in T2av is dominated by iron heterogeneity or some source of error other than noise—a finding consistent with our previous study [5].

There are a number of possible alternatives for breath-held spin-echo T2 mapping. One strategy could be to use a fast-spin-echo approach, where more than one line of k-space is acquired per TE. Unfortunately, this approach would be suboptimal in cases of high iron concentrations. Short T2 values would lead to signal apodization [21] during the echo train. This could cause significant blurring and/or

artifacts. Another strategy for breath-held T2 mapping is the “T2-PREP” approach [22, 23]. In this technique, T₂ contrast is prepared prior to data readout; typically with one or more non-selective RF pulses. The volume magnetization is then stored along the z-axis, after which a slice selective tip-down pulse and a (typically) non-spin-echo readout are used to generate an image of the stored contrast. Subsequent slice-selective pulses are used to capture the contrast in the other slices. A drawback with this approach is that there may be additional T1 contrast generated during the magnetization storage period. Furthermore, the magnitude of T1 contrast will vary between the slices due to the variable magnetization storage time. Also, the contrast may be further altered during the data readout, depending on what acquisition strategy is employed [24]. Another more recent breath-held T2 mapping approach is MR fingerprinting [25]. A detailed comparison with short-TR spin-echo methods in terms of accuracy and precision remains to be performed. An alternate non-spin-echo approach for breath-held LIC quantification is T2* mapping. Several studies have demonstrated good correlation between liver iron content as measured against biopsy [26] and FerriScan [5]. One advantage of T2 over T2* mapping is insensitivity to voxel size and shape, as well as insensitivity to non-iron susceptibility-induced inhomogeneities. However, one clear advantage of T2* methods over (conventional) T2 approaches is their ability

Fig. 6 Comparison of T₂ over the liver between single- and multi-echo techniques for healthy volunteers. Each data point represents the median T₂ value over the liver of one volunteer. Note that the figure is plotted with equal grid spacing on both axes (which accounts for its elongated appearance)

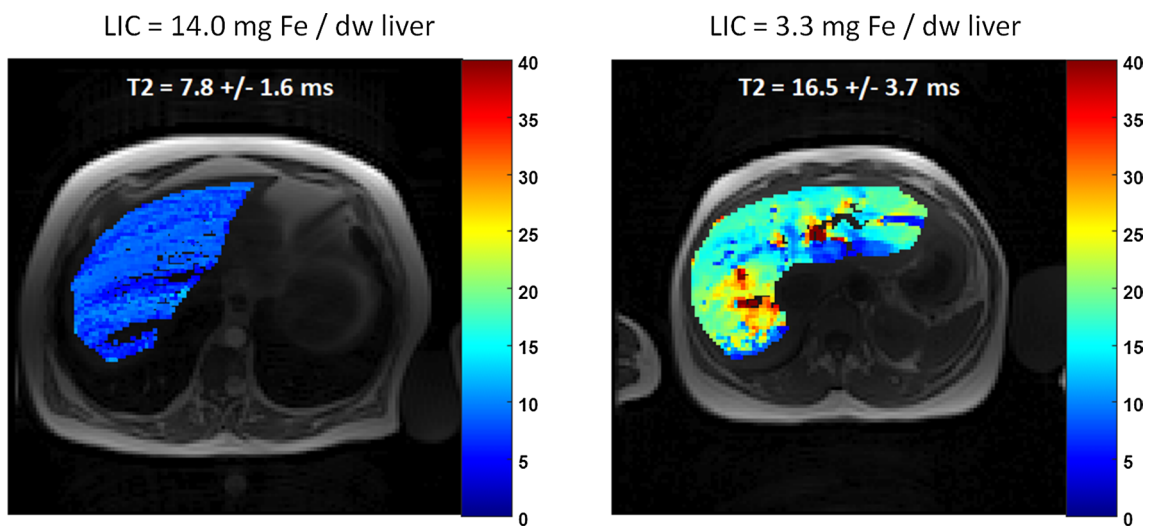
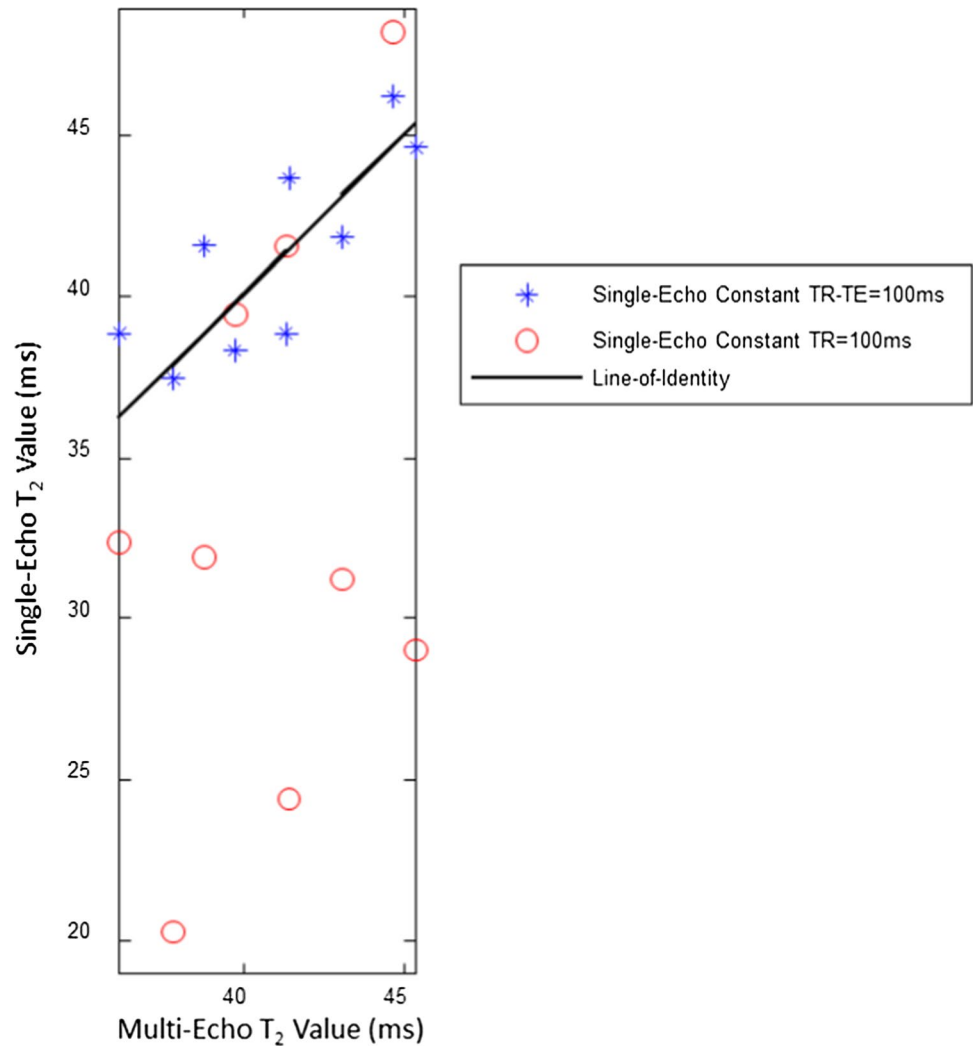


Fig. 7 T₂ maps from two iron overload patients. The liver iron concentration as indicated in the FerriScan reports is listed above each image. Listed T₂ values represent the mean and standard deviation over the liver

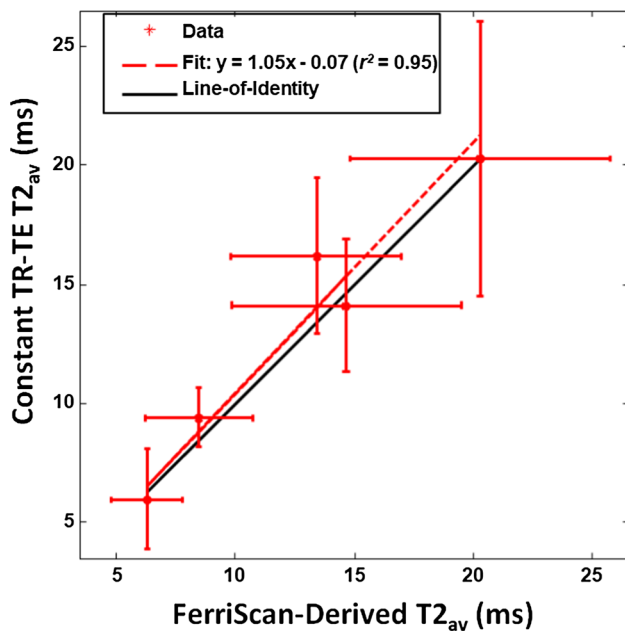


Fig. 8 Comparison of T_{2av} over the liver between constant TR-TE and FerriScan techniques in iron overload patients. The horizontal and vertical error bars represent the standard deviation over the liver ROI for the constant TR-TE and FerriScan techniques respectively

to be performed in a single breath-hold. The current constant TR-TE technique partially mitigates this advantage since it permits breath-hold scanning—though multiple breath-holds are required.

The focus of this study was the single-echo constant TR-TE technique. In healthy volunteers, we used a short TR multi-echo spin-echo pulse sequence that could be performed in a breath-hold for validation. It could be argued that the short TR multi-echo technique could itself be used for assessing LIC. However, several caveats must be mentioned: First, at higher iron loads, the T_2 signal decay behaviour differs for single- and multi-echo techniques [27–30]. Therefore, a separate multi-echo LIC calibration curve would be required. (Note that this differing single/multi-echo decay behavior was not a concern for the healthy volunteers in the present study given their lack of iron). Second, with a short TR multi-slice acquisition, there isn't necessarily an efficiency advantage of a multi-echo vs. a single echo approach. In the case of the former, the TR consists of the acquisition of multiple-echoes from a single slice. In the case of the latter, the TR consists of the acquisition of a single echo from multiple slices. In either case, there is minimal dead time during the TR. As a result, the efficiencies are similar. Another consideration with the multi-echo technique is that hardware and SAR constraints limit the minimum achievable inter-echo spacing. In cases of high iron load, the minimum inter-echo spacing would likely be too long to capture adequately the rapid T_2 decay [28]. On

the other hand, using an approach similar to the constant TR-TE method employed in this study, it is possible to combine together multiple multi-echo acquisitions at different inter-echo spacings [31]. The composite signal generated by combining these multi-echo decays would result in a shorter effective inter-echo spacing. Further investigation into this concept is required.

The advantage of our breath-hold technique over FerriScan's approach is that post-processing to remove respiratory artifacts is not required. However, it should be pointed out that some patients cannot hold their breath. Therefore, the present technique would not be applicable without further post-processing. On the other hand, our technique may be potentially useful in the context of navigated scans. Since each scan may be completed in ~ 20 s, it would be feasible to acquire a relatively large number of successive images that could be potentially used in the context of respiratory gating.

This study had several limitations. First is that it was not possible to generate phantom T_2 values shorter than about 17 ms (whilst maintaining the requisite T_1 range). This corresponds to the mild iron overload range. As discussed previously, achieving shorter phantom T_2 s would have required a higher agar concentration ($>10\%$) than could be achieved. Other studies have utilized phantoms with T_2 values significantly shorter than 17 ms [32, 33]. However, in these studies, shorter T_2 values were associated with shorter T_1 values, which would permit more complete magnetization recovery over the TR. Under these conditions, the constant TR-TE technique would be expected to perform better than the present T_1/T_2 ranges under investigation in this study [10]. However, since this situation is not reflective of iron overload disease, we felt that this would not provide a meaningful (or fair) assessment of the constant TR-TE technique. Another limitation is that there were a relatively small number of volunteers and patients included in this initial pilot study. A larger study involving a more comprehensive comparison between various T_2 and T_2^* techniques is planned. Another limitation of this study is that the focus was on non-fatty livers. Presumably all of the healthy volunteers had non-fatty livers (though this was not measured), and only one of the iron overload patients had a fat fraction greater than 10%. Therefore, the performance of the constant TR-TE technique in fatty livers is unknown. A recent study [34] has demonstrated an increase in the T_1 values of fatty livers to ~ 700 – 1000 ms relative to ~ 600 ms in healthy controls (at 1.5T). T_2 was largely unchanged. In the present context, the increased T_1 values means less complete magnetization recovery, which could potentially lead to a greater T_1 bias. On the other hand, while the T_1 values of the livers assessed in this study were likely closer to the nominal 600 ms range, some of the T_1 phantom values were over 1000 ms (see Table 1). The constant TR-TE technique was able to

provide accurate T2 maps even at these longer T1 values. Another limitation was that volunteer experiments used mono-exponential fits, while patient experiments used bi-exponential fits. In our experience, bi-exponential fits on this type of data are very sensitive to noise, since a four-parameter fit is applied to data with only five TEs. To make bi-exponential fits robust, extensive filtering and pre-processing of the data is required (as per FerriScan's approach [6, 9, 17, 18]). For patients, such pre-processing was unavoidable since the reference standard we used was FerriScan. In volunteers, we preferred to do as little pre-processing as possible to permit a cleaner assessment of the basic technique itself, and not the potentially confounding effects of pre-processing. A desire for minimal pre-processing was also the reason we chose to use the multi-echo spin-echo sequence, rather than FerriScan, for a reference standard in volunteers. A final limitation of this study is that no registration was performed between single-echo images acquired at different TEs. This was done in order to maintain consistency with the FerriScan protocol, which does not do image registration according to published literature (though they do post-process the images to remove ghosting artifacts [8]). To mitigate possible effects of motion, conservative liver ROIs that were away from any non-liver tissue were used. This minimized the likelihood of utilizing pixels with a mixture of liver and non-liver tissue (though this would not reduce the effects of any heterogeneity within the liver).

In conclusion, a short-TR single-echo spin-echo breath-hold technique appears technically feasible for liver T2 mapping. The key to this technique was maintaining a constant TR-TE time for all TE values. Phantom and *in vivo* results demonstrated that this constant TR-TE technique provides T2 estimates with minimal bias using TRs down to approximately 100 ms. In contrast, the conventional approach of maintaining a constant TR for all TEs did exhibit significant bias both in phantoms and *in vivo*. It tended to underestimate the true T2 value.

Author contributions S: Study conception and design, Acquisition of data, Analysis and interpretation of data, Drafting of manuscript, Critical revision. J: Study conception and design, Acquisition of data, Analysis and interpretation of data, Drafting of manuscript, Critical revision.

Funding Funding for this study was generously provided by GE Healthcare.

Data availability Due to privacy concerns, data is not publicly available.

Declarations

Conflict of interest This research was generously supported by GE Healthcare.

Ethical approval This prospective study was performed under Research Ethics Board approval at our institution.

Informed consent Written informed consent was obtained from all participants.

References

- Olivieri NF, Brittenham GM (1997) Iron-chelating therapy and the treatment of thalassemia. *Blood* 89(3):739–761
- Hernando D, Levin YS, Sirlin CB, Reeder SB (2014) Quantification of Liver Iron With MRI: State of the Art and Remaining Challenges. *J Magn Reson Imaging* 40(5):1003–1021
- Runge JH, Akkerman EM, Troelstra MA, Nederveen AJ, Beuers U, Stoker J (2016) Comparison of clinical MRI liver iron content measurements using signal intensity ratios, R (2) and R (2)*. *Abdom Radiol* 41(11):2123–2131
- Wood JC, Enriquez C, Ghugre N, Tyzka JM, Carson S, Nelson MD, Coates TD (2005) MRI R2 and R2* mapping accurately estimates hepatic iron concentration in transfusion-dependent thalassemia and sickle cell disease patients. *Blood* 106(4):1460–1465
- Jhaveri KS, Kannengiesser SAR, Ward R, Kuo K, Sussman MS (2019) Prospective Evaluation of an R2* Method for Assessing Liver Iron Concentration (LIC) Against FerriScan: Derivation of the Calibration Curve and Characterization of the Nature and Source of Uncertainty in the Relationship. *J Magn Reson Imaging* 49(5):1467–1474
- St Pierre TG, Clark PR, Chua-Anusorn W, Fleming AJ, Jeffrey GP, Olynyk JK, Pootrakul P, Robins E, Lindeman R (2005) Non-invasive measurement and imaging of liver iron concentrations using proton magnetic resonance. *Blood* 105(2):855–861
- Sharma SD, Hernando D, Horng DE, Reeder SB (2015) Quantitative susceptibility mapping in the abdomen as an imaging biomarker of hepatic iron overload. *Magn Reson Med* 74(3):673–683
- Clark PR, Chua-anusorn W, St Pierre TG (2004) Reduction of respiratory motion artifacts in transverse relaxation rate (R-2) images of the liver. *Comput Med Imaging Graph* 28(1–2):69–76
- Pavitt HL, Aydinok Y, El-Beshlawy A, Bayraktaroglu S, Ibrahim AS, Hamdy MM, Pang WJ, Sharples C, St Pierre TG (2011) The Effect of Reducing Repetition Time TR on the Measurement of Liver R2 for the Purpose of Measuring Liver Iron Concentration. *Magn Reson Med* 65(5):1346–1351
- Sussman MS, Vidarsson L, Pauly JM, Cheng HLM (2010) A Technique for Rapid Single-Echo Spin-Echo T(2) Mapping. *Magn Reson Med* 64(2):536–545
- Henninger B, Kremser C, Rauch S, Eder R, Zoller H, Finkenstedt A, Michaely HJ, Schocke M (2012) Evaluation of MR imaging with T1 and T2* mapping for the determination of hepatic iron overload. *Eur Radiol* 22(11):2478–2486
- Banerjee R, Pavlides M, Tunnicliffe EM, Piechnik SK, Sarania N, Philips R, Collier JD, Booth JC, Schneider JE, Wang LM, Delaney DW, Fleming KA, Robson MD, Barnes E, Neubauer S (2014) Multiparametric magnetic resonance for the non-invasive diagnosis of liver disease. *J Hepatol* 60(1):69–77
- Tofts PS (2003) *Quantitative MRI of the Brain: Measuring Changes Caused by Disease*. Wiley, Chichester, West Sussex
- Tofts PS, Shuter B, Pope JM (1993) NI-DTPA DOPED AGA-ROSE-GEL - A PHANTOM MATERIAL FOR GD-DTPA ENHANCEMENT MEASUREMENTS. *Magn Reson Imaging* 11(1):125–133
- Gudbjartsson H, Patz S (1995) THE RICIAN DISTRIBUTION OF NOISY MRI DATA. *Magn Reson Med* 34(6):910–914

16. Taylor JR (1982) Taylor JR (1982) An Introduction to Error Analysis: The Study of Uncertainties in Physical Measurements A Series of Books in Physics. University Science Books, Mill Valley, California
17. Clark PR, Chua-anusorn W, Pierre TGS (2003) Bi-exponential proton transverse relaxation rate (R2) image analysis using RF field intensity-weighted spin density projection: potential for R2 measurement of iron-loaded liver. *Magn Reson Imaging* 21(5):519–530
18. St Pierre TG, Clark PR, Chua-anusorn W (2004) Single spin-echo proton transverse relaxometry of iron-loaded liver. *NMR Biomed* 17(7):446–458
19. Bencikova D, Han F, Kannengieser S, Raudner M, Poetter-Lang S, Bastati N, Reiter G, Ambros R, Ba-Ssalamah A, Trattnig S, Krssak M (2022) Evaluation of a single-breath-hold radial turbo-spin-echo sequence for T2 mapping of the liver at 3T. *Eur Radiol* 32(5):3388–3397
20. Idilman IS, Celik A, Savas B, Idilman R, Karcaaltincaba M (2021) The feasibility of T2 mapping in the assessment of hepatic steatosis, inflammation, and fibrosis in patients with non-alcoholic fatty liver disease: a preliminary study. *Clin Radiol* 76(9):709
21. Hennig J, Weigel M, Scheffler K (2003) Multiecho sequences with variable refocusing flip angles: Optimization of signal behavior using smooth transitions between pseudo steady states (TRAPS). *Magn Reson Med* 49(3):527–535
22. Brittain J, Hu BS, Wright GA, Meyer CH, Macovski A, Nishimura DG (1995) Coronary Angiography with Magnetization-Prepared T2 Contrast. *Magn Reson Med* 33:689–696
23. Cassinotto C, Feldis M, Vergniol J, Mouries A, Cochet H, Lapuyade B, Hocquet A, Juanola E, Foucher J, Laurent F, De Ledinghen V (2015) MR relaxometry in chronic liver diseases: Comparison of T1 mapping, T2 mapping, and diffusion-weighted imaging for assessing cirrhosis diagnosis and severity. *Eur J Radiol* 84(8):1459–1465
24. Foltz W, Al-Kwif O, Sussman MS, Stainsby JA, Wright GA (2003) Optimized Spiral Imaging for Measurement of Myocardial T2 Relaxation. *Magn Reson Med* 49(6):1089–1097
25. Jaubert O, Arrieta C, Cruz G, Bustin A, Schneider T, Georgiopoulou G, Masci P-G, Sing-Long C, Botnar RM, Prieto C (2020) Multi-parametric liver tissue characterization using MR fingerprinting: Simultaneous T1, T2, T2*, and fat fraction mapping. *Magn Reson Med* 84(5):2625–2635
26. Garbowski MW, Carpenter JP, Smith G, Roughton M, Alam MH, He TG, Pennell DJ, Porter JB (2014) Biopsy-based calibration of T2*magnetic resonance for estimation of liver iron concentration and comparison with R2 Ferriscan. *J Cardio Magn Reson*. <https://doi.org/10.1186/1532-429X-16-40>
27. Ghugre NR, Coates TD, Nelson MD, Wood JC (2005) Mechanisms of tissue-iron relaxivity: Nuclear magnetic resonance studies of human liver biopsy specimens. *Magn Reson Med* 54(5):1185–1193
28. Doyle EK, Thornton S, Toy KA, Powell AJ, Wood JC (2021) Improving CPMG liver iron estimates with a T-1-corrected proton density estimator. *Magn Reson Med* 86(6):3348–3359
29. Jensen JH, Chandra R (2002) Theory of nonexponential NMR signal decay in liver with iron overload or superparamagnetic iron oxide particles. *Magn Reson Med* 47(6):1131–1138
30. Wang CQ, Reeder SB, Hernando D (2021) Relaxivity-iron calibration in hepatic iron overload: Reproducibility and extension of a Monte Carlo model. *NMR Biomed*. <https://doi.org/10.1002/nbm.4604>
31. Sussman MS A Simple Method for Increasing the Number of Echoes and Decreasing Echo Spacing in T2 Spectrum Analysis. In: ISMRM 19th Annual Meeting & Exhibition, Montreal, Quebec, 2011. p 2752.
32. Wei Z, Ma YJ, Jang H, Yang WH, Du J (2020) To measure T-1 of short T-2 species using an inversion recovery prepared three-dimensional ultrashort echo time (3D IR-UTE) method: A phantom study. *J Magn Reson* 314:106725
33. Sussman MS, Lindner U, Haider M, Kucharczyk W, Hlasny E, Trachtenberg J (2013) Optimizing contrast agent concentration and spoiled gradient echo pulse sequence parameters for catheter visualization in MR-guided interventional procedures: An analytic solution. *Magn Reson Med* 70(2):333–340
34. Erden A, Oz DK, Peker E, Kul M, Ates FSO, Erden I, Idilman R (2021) MRI quantification techniques in fatty liver: the diagnostic performance of hepatic T1, T2, and stiffness measurements in relation to the proton density fat fraction. *Diagn Interv Radiol* 27(1):7–14

Publisher's Note Springer Nature remains neutral with regard to jurisdictional claims in published maps and institutional affiliations.

Springer Nature or its licensor (e.g. a society or other partner) holds exclusive rights to this article under a publishing agreement with the author(s) or other rightsholder(s); author self-archiving of the accepted manuscript version of this article is solely governed by the terms of such publishing agreement and applicable law.